Molecular Basis of Familial Lipoprotein Lipase Deficiency

家族性リポ蛋白リパーゼ欠損症の病因の
分子遺伝学的解明

後藤田　貴也

Molecular Basis of Familial Lipoprotein Lipase Deficiency

家族性リポ蛋白リパーゼ欠損症の病因の分子遺伝学的解明

後藤田　貴　也

Objectives and Background

Familial deficiency of lipoprotein lipase (LPL) is characterized by the extremely severe hypertriglyceridemia, because LPL plays a crucial role in the catabolism of triglyceride-rich lipoprotein particles (1). Familial LPL deficiency is inherited as an autosomal recessive trait and its occurrence has been estimated to be approximately one in a million. The disease usually presents in infancy or childhood with episodic abdominal pain and abnormal appearances of lipemic plasma. The patients have severe chylomicronemia due to a defective hydrolysis of chylomicrons, a marked elevation of fasting serum triglyceride concentrations, and a drastically reduced postheparin plasma LPL activity. Other clinical features of this disease include eruptive xanthoma, lipemia retinalis, hepatosplenomegaly due to the accumulation of chylomicron fat, and recurrent attacks of pancreatitis which are often fatal (2).

The genetic defect responsible for LPL deficiency was not fully elucidated until both the recent molecular cloning of human LPL cDNAs (3,4) and the elucidation of the human LPL gene structure (5) greatly facilitated genomic analysis of the patient genes (6). The human LPL gene has a span of 30 kb and comprises 10 exons that code for a 475-amino acid protein including a 27-amino acid signal peptide. Gene rearrangements of the LPL gene locus were first reported in a population of Caucasian patients (7) and recently several point mutations were also identified in American patients (8-10). To elucidate the molecular basis of the disease and to get a better understanding of the enzyme structure-function relationship, I have investigated the LPL gene of five Japanese patients with no familial relations.

During the analysis of the patient genes, I encountered one splice site mutation. Splice site mutations are common causes of many human genetic

disorders because of a disturbance in the normal processing of pre-mRNA (11). However, precise characterization of the resulting abnormal transcripts has rarely been carried out in vivo, especially when the amount of those transcripts is extremely minute. To gain some insights into the aberrant splicing event in vivo, I carried out the precise characterization and quantitation of aberrantly-spliced mRNAs obtained from an LPL-deficient patient.

Materials and Methods

Patients. We studied five patients and their family members from independent kindreds. A family history of consanguinity was found for each kindred. These patients were diagnosed as LPL deficient by the markedly reduced level of postheparin plasma LPL activity. LPL deficiency was recognized in three of the five patients in infancy, and had been overlooked in the other two until adulthood. One patient (patient 1) was diagnosed at the age of 34 years when he had an attack of acute pancreatitis, and the other patient (patient 4) was asymptomatic but was diagnosed by chance at the age of 42 during examinations for hypertriglyceridemia. The biochemical and physical characteristics of the patients are shown in Table I.

Southern blot analysis. DNAs from the patients and normal subjects were isolated from peripheral white blood cells. Southern blot hybridization analysis was performed after complete digestion of 10 μg of each DNA with one of the restriction enzymes, Hind III, Pst I, Pvu II, Nco I or Bam HI as previously described (6). The 1.58 kb fragment of human LPL cDNA (4) (region 1-1,581) was used as a probe for hybridization.

Northern blot analysis. Total RNAs (30 μg) from both normal subject and the patient 1 were electrophoresed on a 1% agarose gel with 6% formaldehyde, transferred to a nylon membrane, and hybridized with the human LPL cDNA probe (4) at 65°C for one hour. The blot was washed twice with 0.5x SSC-0.1% SDS (1x SSC=150 mM NaCl and 15 mM sodium citrate) at 65°C for 20 min. Hybridization with ß-actin cDNA probe was carried out similarly.

Genomic cloning and gene amplification by the polymerase chain reaction. Construction of genomic libraries was carried out with DNAs obtained from one patient (patient 1) and a normal subject as previously reported (6). By screening the libraries, four LPL gene fragments that cover exons 3 - 9 were obtained from each library. To obtain gene fragments containing exon 1, exon 2, and a portion of exon 10 and to examine the DNA sequences of the LPL gene from the remaining four patients, gene amplification was performed by the polymerase chain reaction (PCR) (12). One μg of each DNA was added to a 100-μl reaction mixture of 50 mM KCl, 10 mM Tris (pH 8.3), 1.5 mM $MgCl_2$, 0.01% gelatin with 0.1 nmol of each primer, 20 nmol of each dNTPs and 2.5 units of Taq DNA polymerase (Perkin-Elmer Cetus). The reaction mixture was applied to 30 cycles of PCR (94°C 1 min; 50-55°C 2 min; 72°C 3 min), which was preceded by an additional denaturation (94°C 5 min) and followed by an extension (72°C 7 min). PCR could properly amplify each of the 10 exons and the adjacent intron sequences. Oligonucleotide primers were synthesized by the phosphoramidite method with the Applied Biosystems model 381A DNA synthesizer.

DNA sequencing. Direct sequencing of amplified DNA was performed utilizing an unequal ratio of primers for the second PCR (13). Following the first PCR, one-hundredth of the reaction mixture was PCR-amplified again as described above, together with an unequal ratio (100 : 1) of the same primers used in the first reaction. The single-stranded DNA from the second PCR was used for sequencing by the dideoxy method (14) after chloroform-extraction and filtration with a Centricon 100 microconcentrator. The cloned gene fragments and the PCR-amplified fragments containing regions with strong secondary structures were sequenced after subcloning into the M13 vector mp18 or mp19.

All sequences were determined on both strands and the regions across a mutation were sequenced on the six independently amplified DNAs.

RFLP-creating PCR. To detect the mutant allele containing the splicing mutation, an artificial restriction fragment length polymorphism (RFLP) was created by introducing a single base mismatch into the 3' portion of an oligonucleotide PCR-primer. A Taq I cutting site was generated specifically in the mutant allele, using the upstream primer whose DNA sequence corresponds to the 3' end of exon 2 (5'- TGGTGATCCATGGCT GGTCG -3'; the mismatched nucleotide is underlined) and the downstream primer corresponding to +98 - +117 of intron 2 (5'- GTAAGAGATCCACGTGAG AT -3'). The sequence of the PCR product derived from the mutant allele was thus modified to contain a new restriction site for Taq I (TCGA) across the exon 2-intron 2 boundary.

Allele-specific oligonucleotide hybridization. One-tenth of the PCR products (10 µl) covering exon 3 were spotted in duplicate on nylon membrane. The DNA blots were hybridized with ^{32}P end-labelled synthetic oligonucleotide probes (normal = 5'- GGAATGTATGAGAGTTG -3'; mutant = 5'- GGAATGTAAGAGAGTTG -3'). Both membranes were washed at 51 °C for 15 min in 6 x SSC-0.1 % SDS.

Site-directed mutagenesis and in vitro expression studies. To construct the normal expression plasmid (pCMV-LPL), human LPL cDNA was placed under the control of the CMV promoter. A 1,581-bp cDNA fragment (4) encompassing the entire coding sequence was cloned in the sense orientation into the Eco RI site of the Bluescript II KS+ vector (Stratagene). The insert was

re-excised with Hind III and Xba I, and transferred to the Hind III/Xba I sites of the Rc/CMV vector (Invitrogen). To construct the mutant expression plasmids, DNA segments containing each of the two missense mutations were generated by PCR and introduced into pCMV-LPL by replacing the corresponding normal segments. For the construction of the mutant plasmid pLPL-His^{243}, the 273-bp DNA fragment (983-1,255) (3) was amplified with the mismatched 5'-primer containing the Arg to His mutation at nucleotide 983 and was introduced into the Eco 47III/Stu I sites of the partially digested pCMV-LPL plasmid. To construct the pLPL-Glu^{204}, the 211-bp DNA fragment (783-993) comprising the Asp to Glu mutation at nucleotide 867 was created by the recombinant PCR method of Higuchi et al. (15), which utilizes two overlapping inside primers containing the same mutation in addition to the outside primers. After digestion with Acc I and Eco 47III, the resulting restricted fragment (792-982) was cloned into the partially digested pCMV-LPL. The integrity of the normal and mutant expression plasmids was verified by DNA sequencing before transfection into COS-1 cells. DNA transfections were carried out using lipofection with TransfectACE (BRL). Thirty hours after each DNA transfection, the medium was supplemented with 5 units/ml of heparin. After an additional 18 hr, the culture medium and cell extract were collected from 35-mm dishes, flash frozen and stored at -70 °C.

Lipoprotein lipase activity and mass. LPL activity in plasma and culture media was determined as described previously (16), using glycerol tri [1-^{14}C] oleate as substrate and selective blocking of the hepatic lipase activity with an antiserum to human hepatic lipase. After an overnight fast, a bolus injection of heparin (10 units/kg) was administered to each subject, and blood was collected 10 min after heparin injection. LPL enzyme mass was measured by a

sandwich enzyme-linked immunosorbent assay (ELISA) recently developed in our laboratory. The ELISA utilizes two separate polyclonal antibodies raised against a synthetic peptide of 16 amino acids corresponding to the N-terminus of the mature human LPL and against a recombinant whole human LPL. Purified human LPL was used as the standard to calculate enzyme mass. In the expression studies, the determination of LPL mass and activity were performed in octuplicates and triplicates, respectively.

Preparation of Monocyte-derived Macrophages. Human monocyte-derived macrophages were prepared by culturing human peripheral monocytes. Mononuclear cells were isolated from peripheral blood cells by the Ficoll-Hypaque gradient method as described previously (17). The cells were washed three times with phosphate-buffered saline (PBS). The washed cells were suspended in RPMI-1640 and plated in 12-well plastic plates (3×10^6 cells/16 mm well). After two hours of incubation at 37°C in 5% CO_2 and 95% air, non-adherent cells were removed by three washes with PBS. The cells were then placed in fresh RPMI-1640 medium supplemented with 10% autologous serum and cultured for one week. The medium was changed twice. The differentiated macrophages were lysed with a 5.5 M guanidine thiocyanate homogenization buffer containing 25 mM sodium citrate (pH 7.0), 0.5% N-lauroylsarcosine, and 0.2 M 2-mercaptoethanol. Total cellular RNA was isolated from the cell lysates by the guanidine thiocyanate method (18).

Reverse Transcription Coupled with PCR Amplification. Total RNA (1 µg) was incubated for 60 min at 37°C in reaction mixture (25µl) containing 50 mM Tris (pH 8.3), 75 mM KCl, 3 mM $MgCl_2$, 10 mM dithiothreitol, 5 nmol of each deoxynucleoside triphosphate (dNTP), 5 units of ribonuclease inhibitor from

human placenta, 100 pmol of random hexamer primers and 200 units of Moloney murine leukemia virus reverse transcriptase (BRL). The total products were subsequently subjected to the first PCR using an equal volume (25μl) of solution containing 50 mM KCl, 10 mM Tris (pH 8.3), 0.01% gelatin, 5 nmol of each dNTP, 5 μl dimethyl sulfoxide, 15 pmol of 5'-primer and 2.5 units of Taq DNA polymerase. PCR-amplification (25 cycles) was performed under the following condition: 1-min denaturation at 94°C, 2-min primer annealing at 50°C and 3-min extension at 72°C. To amplify target regions, 1/1000 of the first PCR products were again subjected to the second PCR with a pair of internal primers.

Results

As shown in Table I, all five patients presented the characteristically severe hypertriglyceridemia and a reduced level of LPL activity. The possibility of the congenital absence of apolipoprotein C-II (19), a co-factor of LPL, could be excluded because of the increased concentration of apolipoprotein C-II observed in all five patients.

Table I. Characteristics of the 5 patients

Subject	Age / Sex*	Triglycerides mg / dl	Total Cholesterol mg / dl	Apolipoprotein C-II mg / dl	LPL activity µmoles / FFA / ml / hour	Clinical Manifestations: Eruptive Xanthoma	Lipemia Retinalis	Pancreatitis	Hepato-splenomegaly
Patient 1	34 / M	4,928	568	9.8	0.8	(−)	(+)	(+)	(−)
Patient 2	3m / F	19,120	824	11.2	0.9	(+)	ND†	(−)	(+)
Patient 3	6m / F	6,010	632	14.8	1.0	(+)	(+)	(−)	(+)
Patient 4	44 / F	1,528	191	6.5	1.2	(−)	(−)	(−)	(−)
Patient 5	23d / F	4,794	560	6.7	1.1	(+)	(+)	(−)	(+)
Normal ¶		40 - 150	130 - 230	3.7 ± 1.3	6.4 ± 2.1				

* m = months, d = days.
† ND, not determined.
¶ Normal values for adult subjects.

In agreement with our previous results with Eco RI (6), Southern blot analysis with five other restriction enzymes showed no evidence of major rearrangement in the LPL gene locus of the patients (data not shown).

Nucleotide sequence of the entire LPL coding region and the exon-intron boundaries was determined for each patient. The results identified five distinct single-base substitutions and confirmed that no other nucleotide alterations are present in the LPL gene of the patients. As expected from the family history of consanguinity, all five patients were found to be homozygous for each point mutation. Figure 1 demonstrates the pairs of sequencing ladders that represent

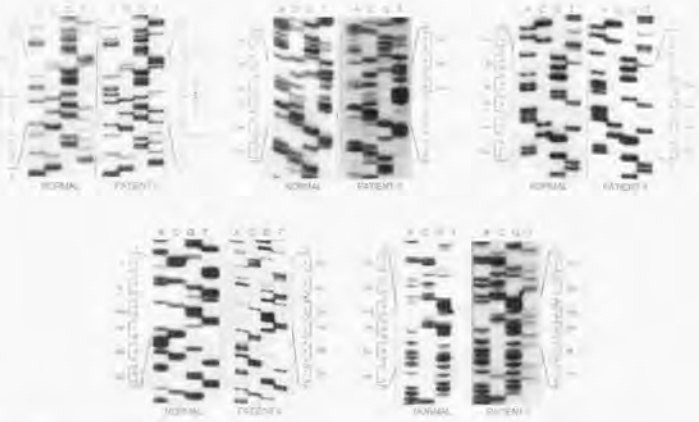

Figure 1. Comparison of DNA sequences from a normal subject and the five patients. All sequences were determined on both strands by direct sequencing of the amplified DNA, and the regions across a mutation were sequenced on the separately amplified DNAs. The sequences of the sense strand (patients 1, 3, 4) or anti-sense strand (patients 2, 5) are shown for comparison. The bases substituted in the patients are enclosed by the box.

sequences from both normal and patient DNA containing the region near the respective mutations. Patient 1 has a G to A change at the first nucleotide of intron 2. This single base change disrupts the invariant GT profile of the eukaryotic 5'-donor splice site (11). Patient 2 has a T to A substitution at Tyr^{61} (TAT), which creates a stop codon (TAA) in exon 3 and would cause a premature termination in LPL synthesis. Another nonsense mutation was identified in the gene of patient 3 who has an A substituting for a G at Trp^{382} (TGG), which also creates a premature termination codon (TGA) in exon 8. Two missense mutations were found in the gene of the remaining two patients. Patient 4 has a C to G transversion that replaces Asp^{204} (GAC) with Glu (GAG) in exon 5 , and patient 5 has a G to A transition that changes Arg^{243} (CGC) to His (CAC) in exon 6. To exclude the possibility of misincorporations during PCR

(12), direct sequencing was performed for each patient's DNA derived from six independent amplifications by separate PCRs.

Of the five point mutations described above, three can affect the restriction sites recognized by the commercially available restriction enzymes. The point mutations in patients 3, 4 and 5 were predicted to disrupt a Mbo II site, a Hinc II site and an Eco 47III site respectively. Thus in these three patients, enzymic digestion was expected to generate a distinctive unique fragment (Fig. 2).

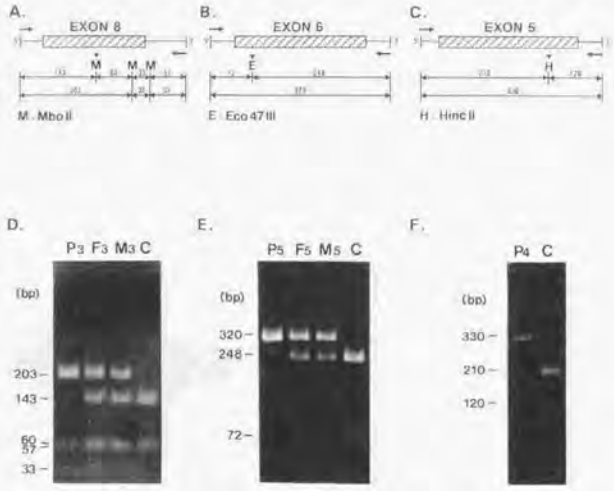

Figure 2. Detection of the three mutations by digestion with restriction enzymes. Schematic representations of the portion of the LPL gene that were amplified by the individual PCR are shown in panels A, B, and C. The pairs of primers used are indicated by the arrows and the positions of normal restriction sites by the vertical lines. The restriction sites disrupted by the mutations are marked with an arrowhead. Numbers indicate the size of the fragments generated by the respective digestions. Electrophoretic analyses of the amplified DNAs from the patients (P), fathers (F), mothers (M) and a normal control (C) were performed with 2% agarose gel after digestion of the DNAs with an appropriate restriction enzyme. As shown in panels D, E, F, the respective unique fragments were demonstrated in the DNAs from the patients, and heterozygous restriction patterns were confirmed for the parents.

Mbo II digestion of the PCR-amplified products of 293 bp generated four fragments of 143, 60, 57 and 33 bp for normal subjects. Instead, similar digestion of the amplified DNA from patient 3 resulted in the occurrence of the unique 203 bp fragment in addition to the common 57 and 33 bp fragments, due to the loss of one of the three internal Mbo II sites (Fig. 2A, 2D). Digestion of the PCR-amplified DNA containing exon 6 with Eco 47III divides the 320 bp products into two fragments of 248 and 72 bp in normal subjects, but a similar digestion did not cleave the amplified DNA from patient 5. This indicates the disruption of the Eco 47 III restriction site by the missense mutation (Fig. 2B, 2E). The fact that patients 3 and 5 did not show any normal size fragment while their parents have both the normal and abnormal size fragments confirmed that they are true homozygotes with the corresponding mutations on both alleles, each of which was inherited from the paternal and maternal pedigree. Hinc II digestion also confirmed homozygosity of patient 4 for the mutation, although the DNA samples from the parents were unavailable (Fig. 2C, 2F).

Since the remaining two mutations cause no change in a restriction site, we developed alternative methods to detect each mutation. The donor splice site mutation was detected by an artificially created Taq I - RFLP which was specifically introduced into the mutant allele (Fig. 3). The result confirmed the homozygosity of patient 1 (P1) and demonstrated that his elder sister (S1-1) who had moderate hypertriglyceridemia with a markedly reduced LPL activity is also a true homozygote for the same splicing mutation. To detect the mutant allele with the nonsense mutation at Tyr^{61}, allele-specific oligonucleotide hybridization was carried out (Fig. 4). The result established the homozygosity of patient 2 (P2) and also demonstrated that, in addition to both parents (F2, M2), her elder sister (S2) as well as another LPL-deficient patient (Pc) is also heterozygous for the same mutation.

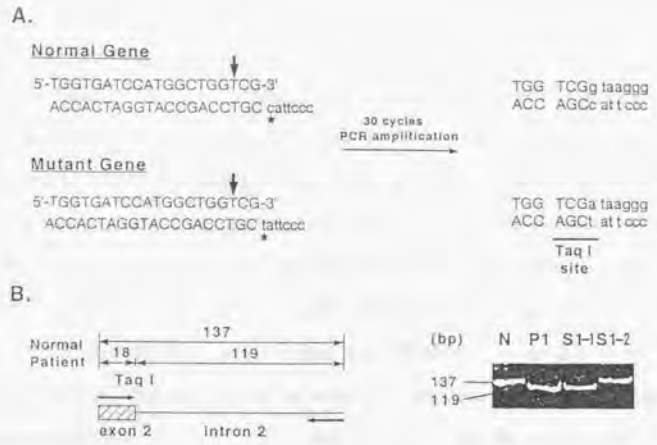

Figure 3. Detection of the splicing mutation by RFLP-creating PCR. (A) The strategy for the specific introduction of an artificial Taq I site into the splicing mutant allele by the RFLP-creating PCR. (B) Taq I-digestion of the amplified DNA from the mutant allele generates the specific 119 bp-fragment, as depicted in the right panel. N, P1, S1-1 and S1-2 denote the normal, patient 1, sister and brother, respectively.

Normal probe : 5'- GGAATGTATGAGAGTTG -3'

Mutant probe : 5'- GGAATGTAAGAGAGTTG -3'

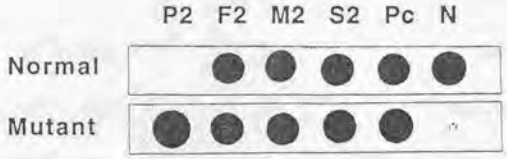

Figure 4. Detection of the nonsense mutation at Tyr^{61} by allele-specific oligonucleotide hybridization. The amplified genomic DNAs containing exon 3 were dot-blotted in duplicates and hybridized with two allele-specific probes for the normal and mutant sequences encompassing the nonsense mutation at Tyr^{61}. P2, F2, M2, S2, Pc and N denote the patient 2, father 2, mother 2, sister 2, compound heterozygote and normal control, respectively.

To investigate the prevalence of the point mutations described above, we examined three additional unrelated patients who had no family history of consanguinity. As shown above, one patient (Pc) was a possible compound heterozygote with only one allele containing the same mutation as patient 2. The other two patients, however, had none of the mutations identified thus far.

The LPL enzyme mass in the postheparin plasma of the patients was measured by an ELISA using polyclonal antibodies raised against human LPL (Table II). Virtually no LPL enzyme mass was detected in plasma from patients 1 and 2, suggesting that the genetic defects in these two patients are null-allelic mutations. Regarding the other three patients, variously decreased but significant levels of LPL mass were found in their postheparin plasma. In contrast, the enzyme mass in the preheparin plasma from the three patients was uniformly at undetectable levels (data not shown).

Table II. LPL enzyme mass in the postheparin plasma of the 5 patients

Patient No.	Mutation	LPL enzyme mass (ng / ml) *	Protein class ‡
Patient 1	GT → AT	2	Class I defect
Patient 2	Tyr^{61} → Stop	0	Class I defect
Patient 3	Trp^{382} → Stop	22	Class II or III defect
Patient 4	Asp^{284} → Glu	118	Class II defect
Patient 5	Arg^{243} → His	84	Class II defect

* Controls (n = 6) : 410 ± 96 (mean ± SD).

‡ Classification of protein defects according to Auwerx et al.

To examine the functional significance of the two missense mutations, expression plasmids coding for the normal LPL (pCMV-LPL) as well as the Glu^{204}- and His^{243}- mutants (pLPL-Glu^{204} and pLPL-His^{243}) were transfected into COS-1 cells, and both the media and the cell homogenates were assayed for LPL mass and activity. Media harvested from cells transfected with the pLPL-Glu^{204} and pLPL-His^{243} mutant plasmids contained decreased levels of LPL mass (26 % and 24 % of the level in normal control, respectively), while such decreases in the level of LPL mass were less significant in the cell homogenates (73 % and 61 % of normal control, respectively) (Fig. 5A).

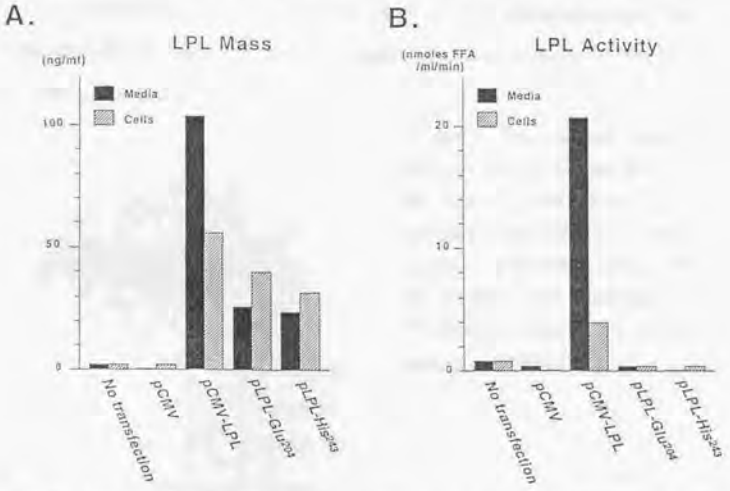

Figure 5. LPL expression in COS-1 cells transfected with the normal and mutant expression vectors. COS cells were transfected with Rc/CMV vector without insert (denoted pCMV), or with pCMV-LPL carrying the normal LPL cDNA, or with pLPL-Glu^{204} carrying the Asp^{204} to Glu mutant cDNA, or with pLPL-His^{243} carrying the Arg^{243} to His mutant cDNA. (A) LPL mass is in nanograms per milliliter. (B) LPL activity is expressed as nanomoles of free fatty acids per milliliter per minute. LPL mass and activity were measured both in the culture medium (solid bars) and in cell homogenates (hatched bars).

Neither of the mutant proteins showed detectable enzymatic activity both in the media and in the cells (Fig. 5B). These data demonstrated that the Asp^{204} to Glu and the Arg^{243} to His mutations both result in the production of LPL molecules which are catalytically defective and are less efficiently secreted from the expressing cells.

Figure 6 represents a three-dimensional structure model of the human LPL which was adapted from the recently published x-ray crystallography of the human pancreatic lipase (20). This model revealed that both amino acid substitutions derived from the two missense mutations should occur in the close proximity of the catalytic center of the enzyme. This observation raises the possibility that those amino acid changes may affect specific constellations around the catalytic site.

Figure 6. Two missense mutations identified near the catalytic triad structure. The three amino acid residues that constitute the catalytic triad are marked with an asterisk, and the two amino acids substituted for by the missense mutations are marked with a closed circle.

Further study was carried out on the LPL mRNA transcripts in the patient 1 who has a donor splice site mutation at the first nucleotide of intron 2 (Fig. 7A).

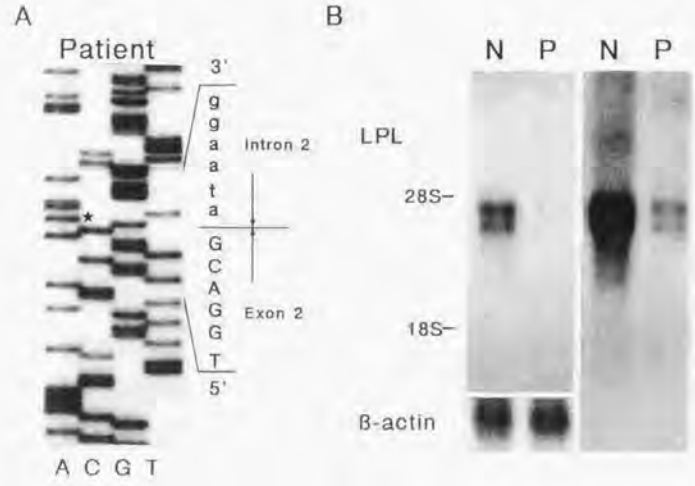

Figure 7. DNA sequence analysis of the patient's LPL gene and Northern blot analysis of macrophage RNA. (A) DNA sequence of the exon 2 - intron 2 boundary in the LPL gene of the patient 1. The G to A substitution in the donor splice site is indicated by an asterisk. (B) Northern blot analysis of monocyte-derived macrophage LPL mRNA. N = normal, P = patient 1. Longer exposure (right) revealed the markedly decreased levels of LPL mRNA in the patient 1.

Northern blot analysis of total RNA from monocyte-derived macrophages revealed a strikingly decreased level of LPL mRNA in the patient 1, while the levels of ß-actin mRNA were the same for normal subject and the patient (Fig. 7B). Despite the decrease in the LPL mRNA level, the length of the LPL mRNA of the patient 1 was almost the same as that of the LPL mRNA of the normal subject. Two species of mRNAs with a length of 3.4 and 3.8 kb, resulting from an alternative utilization of polyadenylation signals (3), were detected in both cases.

To further investigate the LPL mRNAs in the patient 1, PCR technology was adopted for the amplification of the regions of interest within mRNA transcripts.

After reverse transcription of mRNA with random primers (hexamers), the cDNA product was subjected to the first PCR with only a 5'-outer primer (primer A in Fig. 8). Subsequently, 1/1000 of the first reaction product was amplified again by the second PCR with a pair of appropriate internal primers (Fig. 8).

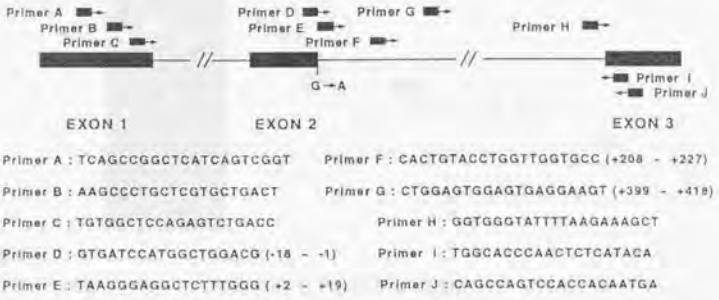

Figure 8. Location and nucleotide sequence of the oligonucleotide primers used for PCR. To examine the possible occurrence of exon skipping, primer C was used in the second PCR together with primer I. Similarly, to examine the possibilities of the activation of cryptic splice sites and the retention of unspliced whole intron 2 in the LPL mRNA transcripts, primers C-G and primer H were used as a 5'-primer. The numbers represented for primers D-G in parentheses indicate the exact position of the nucleotide sequence of respective primers. (+1 denotes the position of the first nucleotide of intron 2.)

Figure 9 shows the results of a second PCR with a pair of oligonucleotide primers (primers C and I in Fig. 8). Staining with ethidium bromide showed a single major band of the expected size for the normal subject, indicating that the PCR accurately amplified the target region of 242 bp length. In contrast, the same PCR gave rise to a 224 bp-, an 18 bp shorter fragment for the patient 1. Since our previous findings had indicated that there is no deletion in the coding region of the patient's gene, this abnormal fragment most likely reflects the

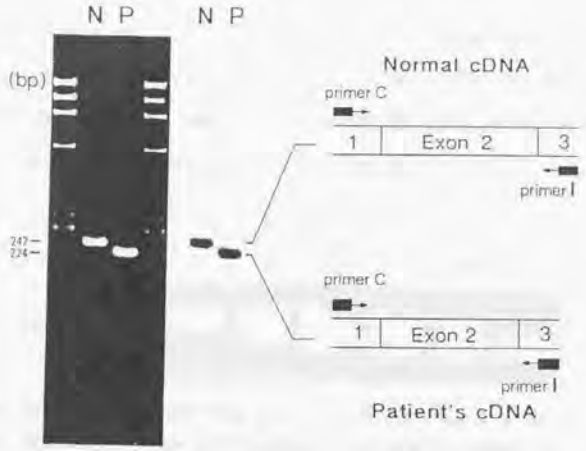

Figure 9. Detection of aberrant splicing in LPL mRNA of the patient 1. PCR amplification with primers C and I yielded fragments of different length in the normal subject and patient's cDNA (N = normal, P = patient 1). Reaction products were analyzed by agarose-gel electrophoresis with DNA molecular size standards (øX174/Hae III) (left) and by Southern blot hybridization with ^{32}P-labeled human LPL cDNA (middle). Schematic representation of the predicted structure of LPL cDNAs from the normal subject and the patient is given in the right panel.

aberrant splicing event in the mRNA of the patient 1. Southern blot analysis, performed with a human LPL cDNA probe confirmed that both the 242 bp and 224 bp fragments were indeed from LPL mRNAs (Fig. 9). These results suggested that the abnormal 224 bp fragment was probably derived from the misspliced LPL mRNA of patient 1 as depicted in the right panel of Fig. 9.

The amount of the abnormal transcript was precisely measured by the competitive PCR method which was recently developed for the quantitation of cytokine mRNA by Gilliland et al. (21). Since both the 242 bp and 224 bp fragments can be co-amplified with the same set of primers and their sizes are only slightly varied, co-amplification of the two fragments should occur in a

concentration-dependent manner. As shown in Fig. 10, the same amount of 242 bp and 224 bp fragments was obtained when cDNAs of the normal subject and the patient were mixed at a ratio of 1:12. The results indicate that the amount of the abnormal transcript is only about 1/12 of that of the normal.

Figure 10. Quantitation of the aberrantly spliced LPL mRNA of patient 1 by the competitive PCR method. Normal cDNA (N) and patient's cDNA (P) were mixed in a series of ratios as indicated, and the mixtures were PCR amplified with primers C and I. The relative amount of the two products reflects the original contents of normal and patient's LPL mRNAs.

Direct sequencing of the 224 bp fragment identified a newly created boundary between exons 2 and 3, which was located 18 bases upstream from the authentic boundary (Fig. 11). The new exon 2-intron 2 junction also contained an alternative GT dinucleotide.

To investigate if the other aberrant splicings could occur at all in vivo, the following experiments were performed. First, I obtained the DNA fragments which migrated faster than the 224-bp fragment in the lane corresponding to patient 1 (Fig. 9). Repeated PCR amplifications of this DNA fraction with primers C and I failed to amplify any specific fragment. The results, therefore, excluded the possibility of exon skipping which joins exons 1 and 3, and activation of cryptic splice sites upstream from the major cryptic site. Next, I performed a second PCR with a new pair of primers D and I (Fig. 8), which indicated the occurrence of downstream splicing sites by evading the major cryptic site involved in the formation of the 224 bp fragment. After the second PCR

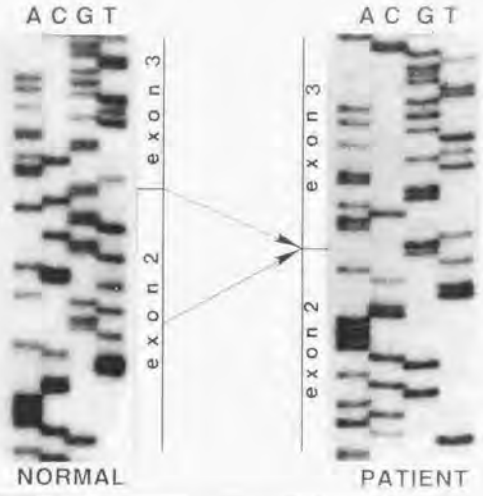

Figure 11. Comparison of the cDNA sequences coding for normal and patient's LPL. Each autoradiogram represents the cDNA sequence encompassing the exon 2- exon 3 boundary of LPL gene. The nucleotide sequence of cDNA from patient 1 revealed an in-frame 18-bp deletion at the 3'-terminus of exon 2.

amplification, four species of fragments were visible in the gel, as shown in Fig. 12. These DNA fragments must have been generated by the activation of the minor cryptic splice sites present in intron 2. The four fragments were separately eluted from the agarose gel and were directly sequenced. These experiments not only identified the exact location of four minor cryptic splice sites (+43, +146, +250, +387 in intron 2), but also confirmed the presence of "alternative GT" within the sequence of the respective sites. Longer exposure of the autoradiograph in Fig. 9 also demonstrated the presence of minor bands with an intensity, as measured by a densitometer, of approximately 1/200 of that of the major band corresponding to the 224 bp fragment. In addition to these four minor sites, more infrequently utilized sites were identified by sequence

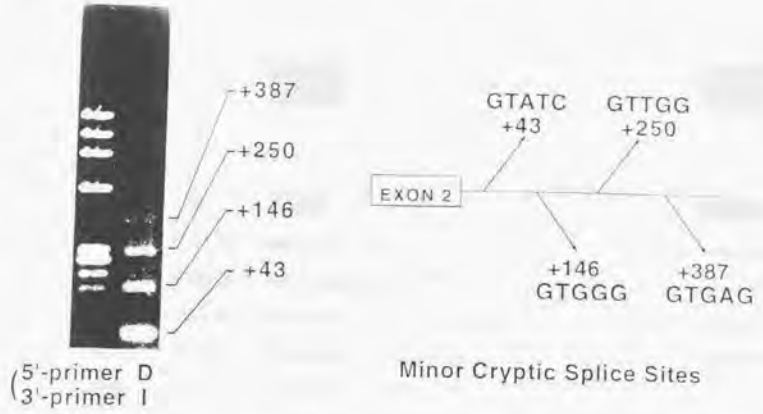

Figure 12. Detection of minor transcripts present in vivo. Four species of fragments derived from patient's cDNA were amplified to a visible state by a second PCR with primers D and I. To avoid amplification of the transcripts made with the major cryptic site, the 5'-primer (primer D) was located immediately downstream of the major site. The number indicated on the right vertical axis represents the position of the cryptic splice sites responsible for the generation of respective fragments. DNA size marker = øX174/Hae III. Schematic representation given in the right illustrates the four minor cryptic splice sites.

analysis of the total PCR products which were subcloned into M13 vectors. Of 100 clones examined, two contained the inserts derived from the activation of sites other than the four minor sites. These results indicated that the patient's LPL mRNA consisted of multiple species of transcripts which resulted from aberrant splicing with various degrees of frequency. To examine the possibility of the occurrence of further downstream splicing, we performed second PCRs with 5'-primers (primers E, F, G and H represented in Fig. 8). However, the results denied the possibility of further downstream splicing as well as the possibility of retention of intron 2 in the mRNA (data not shown).

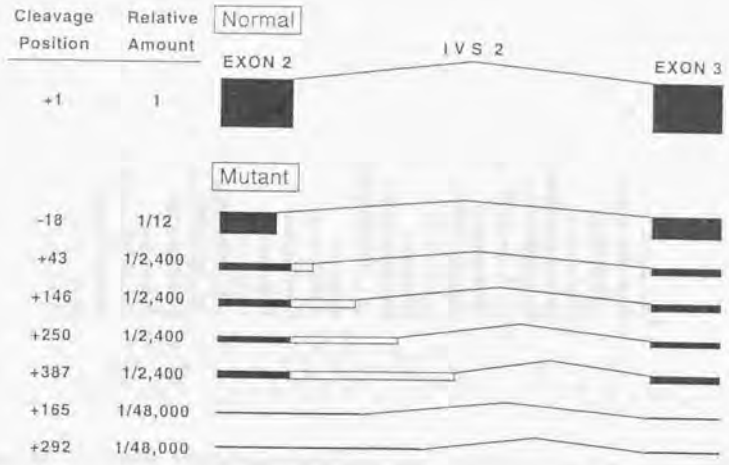

Figure 13. Schematic representation of the splicing events detected for the normal and mutant genes. Relative amounts of the respective transcripts were roughly estimated according to the results of competitive PCR, densitometrical measurement and the frequency of the subcloned PCR products.

Figure 13 illustrates the splicing events which occur in the normal and mutant genes as well as the estimated relative amount of each transcript.

Splicing is mediated by the initial interaction of primary transcripts with U1 small nuclear RNA (snRNA) (11). To gain insight into the mechanism of splice site selection in vivo, we compared the seven cryptic sites described above with other GT-containing sequences in intron 2, with respect to the degree of nucleotide homology, location and their free-energy changes (22) upon binding to U1snRNA. The degree of homology to the other known 5'-splice sites was rated according to the report of Shapiro and Senapathy (23). The results are shown in Fig. 14 along with other possible cryptic site sequences that contain GT dinucleotide.The cryptic sites generally showed more favorable values for splice site selection than the other sequences in the two parameters (homology

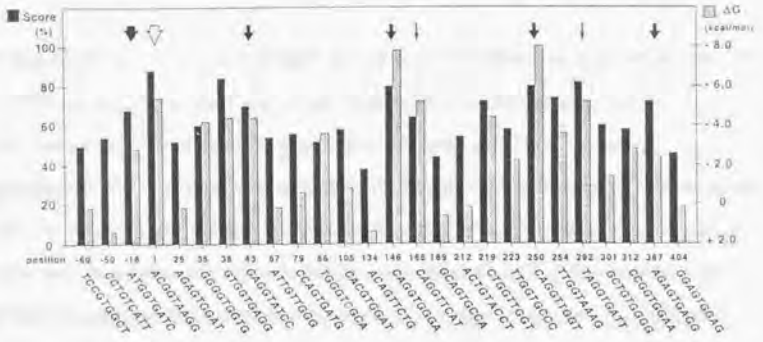

Figure 14. Comparison of the characteristics of potential cryptic splice sites. Scores (solid bars) were calculated according to the method of Shapiro and Senapathy (23) and represent the degree of homology with 5'-splice sites from other genes. ΔG values (hatched bars) were calculated using parameters proposed by Freier et al. (22) and represent the free-energy change upon binding to U1snRNA. Numbers on the horizontal axis indicate the position of the respective GT dinucleotides in intron 2 (position +1 corresponds to the first nucleotide of intron 2, and + symbols are omitted). An open arrow indicates the normal splice site, and three types of solid arrows indicate one major, four minor and two rarer cryptic splice sites.

score and free-energy value). It should be noted that the major cryptic site, although showing unexpectedly unfavorable values for these two parameters, contained the GT dinucleotide nearest to the authentic splice site.

Discussion

In the present study, I described five distinct point mutations responsible for LPL deficiency and developed diagnostic tests for the rapid detection of each mutation. I measured the LPL enzyme mass and performed transient expression of the mutant LPL cDNAs in mammalian cells. I also showed that the LPL mRNAs in patient 1 were misspliced by activation of nearby cryptic splice sites and their amounts were markedly decreased to 1/12 of the normal level. These results not only establish the molecular basis of familial LPL deficiency, but also provide a new insight into the aberrant splicing event in vivo.

At the first nucleotide of intron 2, patient 1 has a G to A substitution that converts the invariant dinucleotides GT into AT in the donor splice site of eukaryotes (11). It is well established that the GT dinucleotides are essential and obligatory for normal splicing of pre-mRNA as they are involved in the correct splice site selection. In fact, we have demonstrated aberrant splicing in this patient, which resulted in decreased levels of LPL mRNA.

In some splicing mutations, two or more cryptic sites are activated simultaneously (24). Furthermore, competition among cryptic sites has recently been demonstrated for the transfected cells by a superb mutagenic technique (25). These findings led me to hypothesize that a series of candidate sequences for cryptic sites might be competitively utilized in vivo, although this competition would be undetectable by conventional methods. To test this hypothesis, I attempted to detect minor transcripts present in vivo in the affected cells of patient 1 with the PCR method. The experiments successfully amplified four minor transcripts to a visible state in gels (Fig. 12). The selection of the minor cryptic sites would not be accidental but would rather follow the same rule that applies to major sites. Indeed, the sequences of all the minor sites showed a

similar degree of favorable values to those of other established splice sites in two parameters (Fig. 14). In addition, the sequence analysis of the subcloned PCR products revealed the presence of two additional rarer transcripts, indicating the possibility that a number of transcripts could exist in vivo at barely detectable levels. These results enabled us to establish a model for 5'-cryptic site selection in vivo whereby a spectrum of sequences can compete with each other for activation and can be utilized at their respective efficiencies. The resultant transcripts are quantitatively so diverse that only a few can normally be found and only some can be detected by PCR, but the majority are undetectable.

Recently, a number of nonsense mutations have been reported to cause a considerable reduction in the corresponding mRNA (26). A reduction in mRNA associated with splicing mutations (27) might be explained partly by a similar mechanism (i.e. mRNA instabilization), because roughly two-thirds of the splicing mutations should alter the reading frame of mRNA, which would introduce a stop codon downstream. The concept was supported by the fact that the splicing mutations with normal levels of mRNA usually cause no frameshift in the coding sequence (24). In contrast, the major change in the LPL mRNA of patient 1 was shown to be a simple in-frame deletion of 18 nucleotides (Fig. 11), however, the amount of the abnormal transcript was greatly reduced to about 1/12 of the normal level (Fig. 10). This reduction can hardly be explained by the extent of the structural change of the transcripts, since the deletional alteration in the present patient is small, and thus is unlikely to seriously affect mRNA stability. One possible explanation is that the binding between the sequences of the major cryptic site in this patient and U1snRNA may be weak. In fact, the predicted free-energy value of the major cryptic site (-2.8 kcal/mol) is not a particularly favorable value for stable binding to U1snRNA (Fig. 14). Since such

binding is one of the rate-limiting steps in RNA processing, instability of the binding would be disadvantageous for sufficient production of mature transcripts.

These results also provide some insight into the factors that affect splice site selection. As has been shown in other studies (24), I found a significant difference in the average values of the two parameters between the seven cryptic site sequences and other candidate sequences (average homology score: 73.6 vs 58.2%; average free-energy value: -5.1 vs -1.7 kcal/mol) (Fig. 14). In the individual case, however, there are some interesting contradictions. For example, the major cryptic site (68.6% and -2.8 kcal/mol) is less favorable than the other minor sites (74.4% and -5.5 kcal/mol in average). In addition, utilization of the sequence GTGGTGAGG at position +38 could not be detected despite the high values in the two parameters. Therefore, in addition to these two parameters, there must be other undetermined factors crucial for splice site selection in vivo. In the selection of the cryptic splice sites, the distance from the authentic site must be another important determinant. In fact, in the present study, we could never detect the activation of the cryptic site farther than +387. The overall RNA structure of the candidate sequences may also be another important factor which should be considered.

LPL is a unique enzyme with multiple functional domains which are postulated to be confined to specific exons. Many investigators assign the asparagine-linked glycosylation site required for the expression of enzyme activity to exon 2, the catalytic serine and the lipid binding domain to exon 4, the highly conserved central domain to exon 5 and the heparin binding site to exon 6 (3,5,28). The introduction of a premature stop codon into exon 3 in patient 2 can thus be easily predicted as exerting the lethal effect on translation. Actually, LPL immunoreactive mass was completely absent in the postheparin plasma of

patient 2, as well as in that of patient 1 (Table II). Thus, these patients exhibit the class I protein defect described by Auwerx et al. (29) which is characterized by null-phenotypic expression.

More informative is the nonsense mutation in patient 3, which occurs in the middle of exon 8 and would terminate translation after synthesizing more than 85% of the normal LPL, including all functional domains noted above. Earlier studies demonstrated that chymotryptic digestion of bovine LPL eliminates the carboxy-terminal portion and causes a loss of activity, not with soluble substrates but with insoluble substrates (30). Recent peptide sequencing analysis of bovine LPL located the chymotrypsin nick immediately after Phe^{390} (the equivalent of Phe^{388} in human LPL) and suggested the succeeding hydrophobic region for another interfacial lipid binding domain (31). Our finding of a nonsense mutation at Trp^{382} in an LPL-deficient patient supports the notion that the carboxy-terminus of LPL is highly important, probably because it is involved in lipid binding. Decreased levels of mRNA, as are often observed in nonsense mutations (26), may also contribute to the LPL deficiency in patients 2 and 3.

Of the 448 amino acid residues consisting of human LPL, only 30 amino acids are completely conserved both among species and among the lipase gene family. The two missense mutations found in patients 4 and 5 both occurred in one of such highly conserved amino acid residues, suggesting an essential role of these amino acids in normal lipolytic function.

The Asp^{204} to Glu substitution in exon 5 of patient 4 is indeed a subtle change with a single methylene addition, but conformation analysis by the Chou and Fasman algorithm (32) predicted that the amino acid change would disrupt a ß-sheet configuration. Furthermore, the base change is not a common polymorphism, because the same base change was not observed in the other

50 alleles examined. Exon 5 encodes the central homologous region which has highly conserved sequences (5). Recently, three missense mutations were identified in exon 5, and the validity of each mutation was confirmed by in vitro expression studies. The Gly^{188} to Glu (8) and Ala^{176} to Thr (9) substitutions both resulted in the synthesis of a catalytically inactive enzyme with a decreased affinity for heparin, and the Ile^{194} to Thr change (10) produced an inactive enzyme with normal heparin affinity. These mutant proteins were present abundantly in the postheparin plasma and were normally expressed in the culture medium of the transfected cells. By contrast, COS-1 cells transfected with the mutant plasmid pLPL-Glu^{204} produced a unique inactive enzyme, which was decreased in amount and was less efficiently secreted from the cells (Fig. 5). In addition, the significant increment in the LPL mass in the patient's postheparin plasma, which is characteristic of the class II defect (29), indicated normal heparin binding of the mutant LPL (Table II). These effects of the mutation at Asp^{204} have more similarities to those of the mutations at Arg^{243} in exon 6 (Fig. 5) rather than to those of the other mutations in exon 5. Therefore, although the dispersion of the mutations in exon 5 (Ala^{176}, Gly^{188}, Ile^{194}, Asp^{204}) implies the presence of an extensive region necessary for normal LPL function, the amino acid substitutions that occur within the same region can cause different effects on the enzyme. It is also noteworthy that the rather conservative amino acid changes at Asp^{204} can abolish LPL function completely. The fact should indicate the extreme intolerance of the LPL molecule to the alterations caused by an amino acid substitution.

The G to A transition in exon 6 of patient 5, which was similarly proved not to be a common polymorphism, also occurs in the highly conserved Arg^{243}. Recently, X-ray crystallographic analysis of human pancreatic lipase revealed that the lipolytic site of the enzyme is formed by a triad structure which is

composed of Ser^{152}, Asp^{176} and His^{263} (equivalent to Ser^{132}, Asp^{156} and His^{241} in human LPL, respectively) (20). Since the Arg^{243} to His substitution occurs close to the His^{241} which is essential for the formation of the catalytic triad, the change is likely to cause the disruption of the enzyme catalytic site (Fig. 6). Expression studies demonstrated that the Arg^{243} to His substitution not only abolishes enzyme activity but also decreases enzyme secretion.

The heterogeneity of familial LPL deficiency has been suggested by biochemical and immunological analyses (2). In this study, I found heterogeneity of this disease also at the molecular level. The diversity of the gene mutation was further supported by the examinations of the three additional patients, which suggested the existence of other undefined mutations even within the relatively homogeneous Japanese population. Without extensive RFLP analyses, DNA haplotyping could not provide useful genetical information regarding LPL deficiency. Identification of a series of naturally occurring mutations, therefore, will be the first step to establish a practical diagnostic system of familial LPL deficiency at the DNA level.

Summary

The DNA sequences were determined for the LPL gene from five unrelated Japanese patients with familial LPL deficiency. The results demonstrated that all five patients are homozygotes for distinct point mutations dispersed throughout the LPL gene.

Patient 1 has a G to A transition at the first nucleotide of intron 2. Northern blot analysis of this patient's RNA showed strikingly low levels of LPL-specific mRNAs. Detailed analysis of the abnormal RNA splicing demonstrated that no normal splicing occurred at the authentic splice site, rather a cryptic splice site 18 bases upstream from the mutation site was preferentially utilized. Although the resulting alteration in mRNA was a minute in-frame 18 base deletion, the amount of the abnormal transcript was only 1/12 that of the normal. In addition to this major cryptic splice site, we also identified multiple minor sites which were utilized at extremely lower efficiencies. The sequences of these minor cryptic sites possessed many of the characteristics common to those of other normal splice sites, indicating that even such minor sites should have also been selected according to the general rules for splice site selection. These results demonstrate that, upon mutation, a broad spectrum of cryptic splice sites are activated in vivo at their respective efficiencies.

Patient 2 has a nonsense mutation in exon 3 (Tyr^{61} to Stop) and patient 3 in exon 8 (Trp^{382} to Stop). The latter mutation emphasizes the importance of the carboxy-terminal portion of the enzyme in the expression of LPL activity. Missense mutations were identified in patient 4 (Asp^{204} to Glu) and patient 5 (Arg^{243} to His) in the strictly conserved amino acids. Expression study of both mutant genes in COS-1 cells produced inactive enzymes, establishing the functional significance of the two missense mutations. In these patients,

postheparin plasma LPL mass was either virtually absent (patients 1 and 2) or significantly decreased (patients 3 - 5). To detect these mutations more easily, we developed a rapid diagnostic test for each mutation. These results not only demonstrate that familial LPL deficiency is a heterogeneous genetic disease caused by a wide variety of gene mutations, but also provide a new tool to examine subjects in the general population who have idiopathic hyperlipidemia.

Acknowledgment

The author would like to thank Drs. Nobuhiro Yamada, Toshio Murase, Fumimaro Takaku, and Yoshio Yazaki for invaluable advice and encouragement.

REFERENCES

1. Garfinkel, A. S., and Schotz, M. C. (1987) in *Plasma Lipoproteins* (Gotto, A. M., Jr., ed) pp. 335-357, Elsevier, New York

2. Brunzell, J. D. (1989) in *The Metabolic Basis of Inherited Disease* (Scriver, C. R., Beaudet, A. L., Sly, W. S., and Valle, D., eds) 6th Ed., pp. 1165-1180, McGraw-Hill, New York

3. Wion, K. L., Kirchgessner, T. G., Lusis, A. J., Schotz, M. C., and Lawn, R. M. (1987) *Science* **235**, 1638-1641

4. Gotoda, T., Senda, M., Gamou, T., Furuichi, Y., and Oka, K. (1989) *Nucleic Acids Res.* **17**, 2351

5. Deeb, S.S., and Peng, R. (1989) *Biochemistry* **28**, 4131-4135

6. Gotoda, T., Senda, M., Murase, T., Yamada, N., Takaku, F., and Furuichi, Y. (1989) *Biochem. Biophys. Res. Commun.* **164**, 1391-1396

7. Langlois, S., Deeb, S., Brunzell, J.D., Kastelein, J.J., and Hayden, M.R. (1989) *Proc. Natl. Acad. Sci. USA.* **86**, 948-952

8. Emi, M., Wilson, D. E., Iverius, P.-H., Wu, L., Hata, A., Hegele, R., Williams, R. R., and Lalouel, J.-M. (1990) *J. Biol. Chem.* **265**, 5910-5916

9. Beg, O. U., Meng, M. S., Skarlatos, S. I., Previato, L., Brunzell, J. D., Brewer, H. B., Jr., and Fojo, S. S. (1990) *Proc. Natl. Acad. Sci. USA* **87**, 3474-3478

10. Dichek, H. L., Fojo, S. S., Beg, O. U., Skarlatos, S. I., Brunzell, J. D., Cutler, G. B., Jr., and Brewer, H. B., Jr. (1991) *J. Biol. Chem.* **266**, 473-477

11. Padgett, R. A., Grabowski, P. J., Konarska, M. M., Seiler, S., and Sharp, P. A. (1986) *Annu. Rev. Biochem.* **55**, 1119-1150

12. Saiki, R. K., Gelfand, D. H., Stoffel, S., Scharf, S. J., Higuchi, R., Horn, G. T., Mullis, K. B., and Erlich, H. A. (1988) *Science* **239**, 487-491

13. Gyllensten, U. B., and Erlich, H. A. (1988) *Proc. Natl. Acad. Sci. USA* **85**, 7652-7656

14. Sanger, F., Nicklen, S., and Coulson, A. R. (1977) *Proc. Natl. Acad. Sci. USA* **74**, 5463-5467

15. Higuchi, R. (1990) in *PCR Protocols : A Guide to Methods and Applications* (Innis, M.A., Gelfand, D.H., Sninsky, J.J., and White, T.J., eds) pp. 177-183, Academic Press, Inc. San Diego

16. Murase, T., Yamada, N., Ohsawa, N., Kosaka, K., Morita, S., and Yoshida, S. (1980) *Metabolism* **29**, 666-672

17. Ishibashi, S., Inaba, T., Shimano, H., Harada, K., Inoue, I., Mokuno, H., Mori, N., Gotohda, T., Takaku, F., and Yamada, N. (1990) *J. Biol. Chem.* **265**, 14109-14117

18. Chirgwin, J. M., Przybyla, A. E., MacDonald, R. J., and Rutter, W. J. (1979) *Biochemistry* **18**, 5294-5299

19. Breckenridge, W.C., Little, J.A., Steiner, G., Chow, A., and Poapst, M. (1978) *N. Engl. J. Med.* **298**, 1265-1273

20. Winkler, F.K., D'Arcy, A., and Hunziker, W. (1990) *Nature (Lond.).* **343**, 771-774

21. Gilliland, G., Perrin, S., Blanchard, K., and Bunn, H. F. (1990) *Proc. Natl. Acad. Sci. USA* **87**, 2725-2729

22. Freier, S. M., Kierzek, R., Jaeger, J. A., Sugimoto, N., Caruthers, M. H., Neilson, T., and Turner, D. H. (1986) *Proc. Natl. Acad. Sci. USA* **83**, 9373-9377

23. Shapiro, M. B., and Senapathy, P. (1987) *Nucleic Acids Res.* **15**, 7155-7174

24. Kuivaniemi, H., Kontusaari, S., Tromp, G., Zhao, M., Sabol, C., and Prockop, D. J. (1990) *J. Biol. Chem.* **265**, 12067-12074

25. Nelson, K. K., and Green, M. R. (1990) *Proc. Natl. Acad. Sci. USA* **87**, 6253-6257

26. Baserga, S. J., and Benz, E. J., Jr. (1988) *Proc. Natl. Acad. Sci. USA* **85**, 2056-2060

27. Treisman, R., Orkin, S. H., and Maniatis, T. (1983) *Nature* **302**, 591-596

28. Semenkovich, C.F., Luo, C.-C., Nakanishi, M.K., Chen, S.-H., Smith, L.C., and Chan, L. (1990) *J. Biol. Chem.* **265**, 5429-5433

29. Auwerx, J.H., Babirak, S.P., Fujimoto, W.Y., Iverius, P.-H., and Brunzell, J.D. (1989) *Eur. J. Clin. Invest.* **19**, 433-437

30. Bengtsson-Olivecrona, G., Olivecrona, T., and Jornvall, H. (1986) *Eur. J. Biochem.* **161**, 281-288

31. Yang, C.-Y., Gu, Z.-W., Yang, H.-X., Rohde, M.F., Gotto, A.M., Jr., and Pownall, H.J. (1989) *J. Biol. Chem.* **264**, 16822-16827

32. Chou, P.Y., and Fasman, G.D. (1978) *Adv. Enzymol.* **42**, 45-148

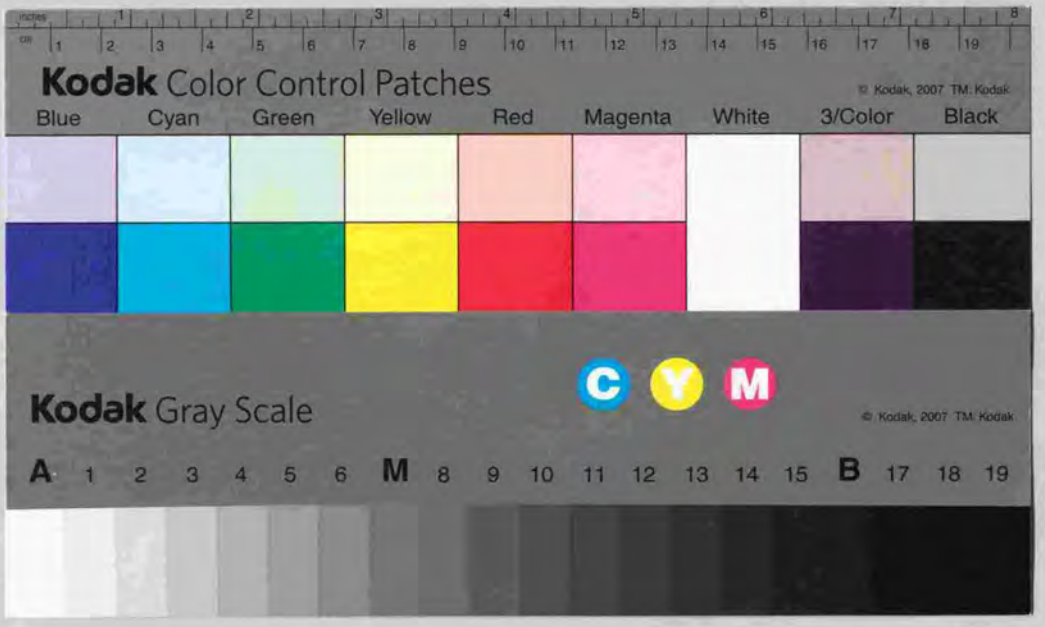
inches
cm
Kodak Color Control Patches
© Kodak, 2007 TM: Kodak
Blue
Cyan
Green
Yellow
Red
Magenta
White
3/Color
Black
Kodak Gray Scale
C
Y
M
© Kodak, 2007 TM: Kodak
A
M
B